forests

MDPI

Article

In Situ Quantification of Root Exudates in a Subtropical Mangrove (*Bruguiera gymnorhiza*) Forest

Norihiro Kato [1], Ken'ichi Osaka [2], Nada Yimatsa [3], Toshiyuki Ohtsuka [3] and Yasuo Iimura [2,*]

[1] Graduate School of Environmental Science, The University of Shiga Prefecture, 2500 Hassakacho, Hikone 522-8533, Shiga, Japan; tz14nkato@ec.usp.ac.jp
[2] School of Environmental Science, The University of Shiga Prefecture, 2500 Hassakacho, Hikone 522-8533, Shiga, Japan
[3] Institute for Advanced Study, Gifu University, 1-1 Yanagito, Gifu 501-1193, Japan; ohtsuka.toshiyuki.p9@f.gifu-u.ac.jp (T.O.)
* Correspondence: iimura.y@ses.usp.ac.jp

Abstract

Root exudates represent a critical belowground carbon flux; however, direct field-based quantification of these rates on intact mangrove roots remains limited due to methodological challenges. Here, we present, to our knowledge, the first in situ evaluation of root exudation rates in a subtropical *Bruguiera gymnorhiza* forest in Japan, employing a modified cuvette method specifically designed for field measurements on intact root systems. The net root exudation rates measured in artificial seawater at depths of 0–60 cm ranged from 0.01 to 0.97 mg C g^{-1} h^{-1}, with a mean of 0.22 mg C g^{-1} h^{-1}. Although this mean rate was comparable to values reported for tropical terrestrial forests, the spatiotemporal variation exhibited variable site-specific patterns. At the midstream site, exudation rates were closely coupled with fine root biomass under nitrogen-limited conditions and peaked during summer. In contrast, the upstream site exhibited unusually high exudation rates during winter, even in deep soil layers. Furthermore, contrary to patterns typically observed in terrestrial forests, exudation rates showed positive correlations with root C:N ratios and proton efflux. These findings suggest that root exudation in mangroves is regulated by complex interactions among site-specific hydrological regimes and stress-adaptation mechanisms, particularly salinity tolerance and nutrient acquisition, rather than by simple growth trade-offs. When integrated over a depth of 0–60 cm, the estimated annual root exudate carbon flux was approximately 0.4 kg C m^{-2} yr^{-1}. This likely represents a conservative lower-bound estimate because fine root systems extend well below this depth in mangrove forests. Our results strongly suggest that root exudates constitute an important, previously under-recognized component of the "missing carbon" in mangrove ecosystems and underscore the need to explicitly incorporate this flux into blue carbon models to more accurately evaluate mangrove carbon sequestration capacity.

Keywords: root exudate; mangrove forests; blue carbon; belowground carbon; *Bruguiera gymnorhiza*

Check for updates

Academic Editor: Xiankai Lu

Received: 26 December 2025
Revised: 19 January 2026
Accepted: 22 January 2026
Published: 24 January 2026

Copyright: © 2026 by the authors. Licensee MDPI, Basel, Switzerland. This article is an open access article distributed under the terms and conditions of the Creative Commons Attribution (CC BY) license.

1. Introduction

In forest ecosystems, fine roots (diameter < 2 mm) continuously release root exudates into the surrounding soil, providing a critical source of labile carbon (C) to the belowground environment. These compounds stimulate soil microbial metabolism [1,2] and can account for up to 20% of net primary production (NPP) in temperate and tropical forests [3–6],

thereby constituting a major component of belowground C flux [7]. Root exudates are dominated by low-molecular-weight compounds such as sugars, organic acids, and amino acids [1,8], which play both quantitative and qualitative roles in driving the "priming effect". This process stimulates the microbial decomposition of soil organic matter—including old, recalcitrant C reserves—across diverse ecosystems such as forests, grasslands, wetlands, and peatlands [9–12]. More recently, the "paradox of soil organic carbon (SOC) stabilization and destabilization" has been proposed, in which root exudate-mediated microbial processes promote both the formation and breakdown of mineral-associated organic carbon (MAOC) [2]. Consequently, root exudates are increasingly recognized as key regulators of soil C dynamics [13–16].

Quantitative assessments of root exudates in forests have largely relied on in situ measurements of mass-specific root exudation rates using cuvette-based techniques [4,17]. These studies have examined spatial variation with soil depth [18–21], seasonal variation [22–24], and relationships with soil physicochemical properties—such as pH, moisture, C:N stoichiometry, nutrient availability, microbial communities, and enzyme activities [20,22,23,25]. Root exudation has also been linked to fine root morphological traits including diameter, specific root length (SRL), specific root area (SRA), root tissue density (RTD), and root C:N ratios [20,25–28]. Although in situ measurement protocols are now established, methodological constraints and logistical difficulties mean that field-based studies remain relatively scarce [7,17,29].

Mangrove forests, despite covering only approximately 0.5% of global coastal area [30], are among the most carbon-rich coastal ecosystems owing to their unique SOC stabilization processes [31,32]. They account for 10–15% of sedimentary carbon storage in coastal regions [30] and play an important role as "blue carbon" ecosystems through the export and sequestration of dissolved inorganic carbon (DIC) derived from SOC mineralization and groundwater inputs [33,34]. Their high C sequestration capacity is supported by high NPP—comparable to that of tropical forests—and, notably, by the strong allocation of C belowground, where fine-root production typically accounts for 30–40% of NPP [35–37]. Meta-analyses indicate that more than 90% of SOC stored in mangrove subsurface layers originates from roots [38], reflecting high fine-root turnover [39,40], deep root penetration beyond 1 m [41–44], and tight coupling with nutrient dynamics [39,45]. In addition, periodic tidal inundation induces strong spatiotemporal variability in soil redox conditions and porewater chemistry, including salinity and oxygen availability [46–48], which in turn influences fine-root production and biomass distribution [38,49]. These features suggest that belowground C dynamics in mangrove forests operate under highly dynamic and site-specific environmental controls.

Although quantitative evaluations of mangrove C fluxes—such as litterfall, wood production, soil CO_2 efflux, and DIC export—have advanced substantially in recent decades [36,37], in situ quantitative data on root exudates remain virtually non-existent [38]. To the best of our knowledge, this belowground C flux remains a major "black box" in mangrove carbon budgets. This knowledge gap likely reflects the strong hydrological disturbance imposed by tidal flooding, which hinders the application of conventional cuvette-based methods in the field. Laboratory studies using mangrove seedlings have elucidated the chemical composition of root exudates [50–52], their interactions with rhizosphere microbial communities [53], and their influence on SOC stabilization and metal dynamics [54,55]. Model-based experiments have further demonstrated that mangrove soil SOC mineralization and DIC production are enhanced through exudate-induced priming effects [56]. However, these findings are limited to controlled conditions, and field-based quantitative assessments are critically lacking.

Given this background, quantitative evaluation of root exudates in mangrove forests is essential for improving our mechanistic understanding of belowground C dynamics and for constraining root-derived C fluxes in blue-carbon assessments. Furthermore, root exudates represent one of the critical components with the potential to bridge the discrepancy between carbon inputs and outputs in current blue carbon models for mangrove forests [33]. Therefore, the quantitative assessment of these exudates is of paramount importance for a more precise and comprehensive understanding of the overall carbon cycle in mangrove ecosystems. In this study, we conducted, to our knowledge, the first in situ quantitative evaluation of root exudates in a pristine mangrove forest in southwestern Japan. Our objectives were to (i) quantify potential root exudation rates of *Bruguiera gymnorhiza*, (ii) assess their spatial and seasonal variation across sites and soil depths, and (iii) explore potential correlations with soil chemical properties and fine-root traits. Through this approach, we aimed to identify the key factors regulating root exudation in mangrove forests and to provide baseline information necessary to incorporate root-derived carbon into mangrove carbon budgets.

2. Materials and Methods

2.1. Study Site

This study was conducted in a pristine mangrove forest located at the estuary of the Gaburumata River in northern Ishigaki Island, Okinawa Prefecture, southwestern Japan (Figure 1a). According to the Japan Meteorological Agency, the site (24°20′ N, 124°09′ E) has a subtropical climate, with a mean annual temperature of 24.9 °C, a mean annual humidity of 77%, and a mean annual precipitation of 2097 mm, based on averages for the period 2020–2024. Figure 1b shows the monthly mean values. The mangrove forest covers approximately 1.0 ha around the river mouth and is dominated by *Bruguiera gymnorhiza*, whereas *Rhizophora stylosa* is sparsely distributed along the seaward fringe. The mean diameter at breast height (DBH) of *B. gymnorhiza* at the midstream and upstream sampling sites (see Section 2.2 for details) was approximately 20 cm, with no apparent difference between the sites. Visual observations indicated that tree sizes in the downstream area were relatively smaller (approximately 15 cm in DBH) than those in the midstream and upstream areas.

The study site is influenced by a semidiurnal tidal regime. Because the topographic relief is minimal, with an elevation difference of less than 1 m across the forest [57], the soil surface is exposed throughout the site during low tide, while seawater inundates even the upstream areas during high tide. All root exudate measurements were conducted during neap tides, when the tidal range was relatively small. During the sampling periods, high and low tide levels ranged from 104–154 cm and 41–99 cm, respectively, in February 2025 (winter), and from 166–174 cm and 62–119 cm in July 2025 (summer). These seasonal differences in tidal ranges likely affected the inundation duration at each sampling location (Figure 1a).

2.2. Root Exudation Measurements and Root C and N Analysis

Root exudates were collected using a modified cuvette-based method based on the design of Phillips et al. [4]. To access the root systems of *B. gymnorhiza*, soil pits of approximately 1 m^3 (1 m × 1 m × 1 m) were excavated at both the upstream and midstream sites. In Japanese subtropical mangrove forests, aboveground productivity (litterfall) has been reported to increase in summer compared to winter, and fine root production has been shown to peak between February and April [58,59]. Furthermore, meta-analyses indicate that mangrove net primary production (NPP) is positively correlated with temperature and precipitation [37]. Accordingly, to capture these contrasting seasonal and biological

variations, measurements were carried out during low tides between 4–7 February 2025 (winter) and 17–20 July 2025 (summer). To represent the soil profile where fine root density typically peaks [41,58], sampling was conducted at two depths: surface (0–30 cm) and deep (30–60 cm) (Figure 1a).

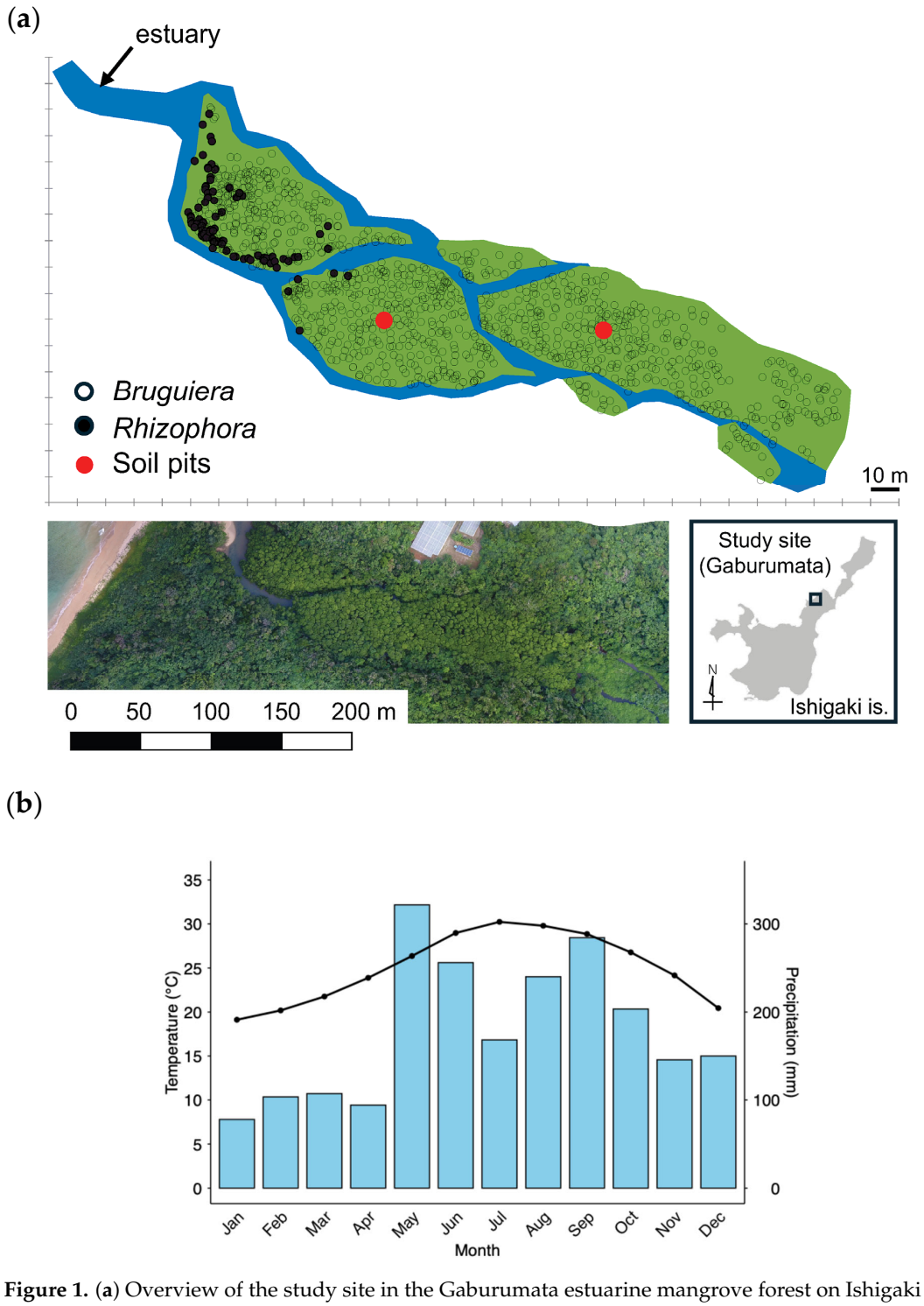


Figure 1. (**a**) Overview of the study site in the Gaburumata estuarine mangrove forest on Ishigaki Island, Japan. Open and black circles represent the distributions of *Bruguiera gymnorhiza* and *Rhizophora stylosa*, respectively; *B. gymnorhiza* dominates most of the forest area. Red circles indicate the locations of soil pits at the midstream and upstream sites. The (**lower panel**) shows a drone aerial view of the site. The study site map was redrawn based on information provided in Ref. [56]. (**b**) Monthly mean temperature and precipitation at Ishigaki Island, Okinawa, Japan, from 2020 to 2024. The line and bars represent temperature and precipitation, respectively.

Fine roots (<2 mm in diameter) still attached to the parent tree were carefully excavated from the soil profile, and adhering soil particles were gently washed off using bottled mineral water. Finally, the roots were rinsed with carbon-free artificial seawater (ASW) to ensure they were equilibrated with the incubation medium. Cleaned fine roots were placed inside 50-mL sterile syringes (Terumo, Tokyo, Japan) and sealed with rubber stoppers. Carbon-free ASW prepared following Deslouis et al. [60] was used as the incubation medium, with the following composition: NaCl 0.25 M, $NaHCO_3$ 1.0×10^{-3} M, Na_2CO_3 1.0×10^{-4} M, $CaCl_2$ 6.94×10^{-3} M, and $MgCl_2$ 5.87×10^{-2} M. The electrical conductivity (EC) of the ASW was adjusted by dilution to match porewater EC at each site. The prepared ASW was filled into syringes and measured after 24 h as a control (without roots); the mean DOC concentration, pH, and EC were 0.6 mgC L^{-1}, 7.54, and 33.1 mS cm^{-1}, respectively.

While the original method by Phillips et al. [4] utilizes a low-concentration nutrient solution, we employed carbon-free artificial seawater to match the in situ saline environment of mangroves. This modification was made because osmotic gradients are known to significantly influence exudation rates in halophytes. Although small glass beads are sometimes used in cuvette-based methods to mimic the physical soil matrix, we omitted them to avoid potential underestimation of carbon flux caused by the adsorption of exudate compounds onto bead surfaces [4]. Moreover, field operations in mangrove forests are strictly constrained by tidal cycles, requiring the installation of syringes within a narrow time window during low tide. To maximize the number of replicates under these time constraints, it was essential to ensure that the installation process was as simple and rapid as possible. Additionally, given the lack of prior data on expected root exudate concentrations, maximizing the recovery volume of the incubation solution was crucial to ensure sufficient sample for analysis. Considering these logistical and analytical requirements, we opted to omit the use of glass beads to streamline field procedures and ensure adequate sample recovery. Beyond these matrix considerations, empirical observations indicated that mangrove fine roots are highly branched and fragile (Figure A2), making physical damage during encapsulation and seawater contamination during high tides the primary technical challenges. To address these, we modified the rubber syringe stoppers with several incisions to facilitate root insertion without mechanical stress. Additionally, the syringes were filled to capacity with the incubation solution (leaving as little headspace as possible) to maintain internal pressure, thereby physically preventing the intrusion of external seawater during tidal inundation (Figure A1).

To minimize physiological stress caused by excavation, 50 mL of ASW was injected into each syringe and a 24-h pre-incubation step was performed. The syringes were then flushed and refilled with fresh ASW for a second 24-h incubation period. Syringes were secured to the soil profile with wire to prevent displacement due to buoyancy during high tide. Control syringes containing only ASW (n = 3) were placed in the surface soil at the midstream site. Sample sizes were as follows: winter—midstream n = 6, upstream n = 10; summer—midstream n = 10, upstream n = 10. In addition, to evaluate the potential effect of solar radiation on exudation, two randomly selected syringes at the surface layer of each site were wrapped in aluminum foil during the July 2025 experiment.

Immediately after retrieval, the pH and EC of the incubation solutions were measured using portable meters (LAQUAtwin pH-11B and EC-33B, HORIBA, Kyoto, Japan). Solutions were then filtered through 0.45 µm cellulose acetate sterile syringe filters (DIMIC CS, ADVANTEC, Tokyo, Japan), transported to the laboratory under refrigerated conditions (4 °C), and analyzed within one week. Total organic carbon (TOC) concentrations were determined using a TOC analyzer (TOC-L, Shimadzu, Kyoto, Japan) in non-purgeable organic carbon (NPOC) mode.

Fine roots recovered from the syringes were rinsed with deionized water, oven-dried at 75 °C for 48 h, and weighed to determine dry mass. Dried samples were ground using a vibrating mill, and their C and N concentrations were measured using a CN analyzer (Sumigraph NC-TR22, Sumika Chemical Analysis Service, Osaka, Japan).

Mass-specific root exudation rates (mg C g root^{-1} h^{-1}) were calculated by subtracting TOC values of the controls from those of the treatment syringes, and dividing by root biomass (g) and incubation time (h). This value represents a net exudation flux, as it integrates exudation, potential reabsorption by roots, and microbial decomposition during incubation.

2.3. Fine Root Biomass Measurements

Fine root biomass was measured at the midstream site in late January and July 2025. Soil cores were collected from three depth intervals (0–15, 15–30, and 30–50 cm) using a Russian-type open-face peat sampler (DIK-105A, Daiki Rika Kogyo Co., Ltd., Saitama, Japan) with a cross-sectional area of 9.8 cm^2. The discrepancy in sampling depths (30–60 cm for exudates vs. 30–50 cm for biomass) arose because fine-root biomass was collected at fixed intervals of 0–15, 15–30, 30–50, and 50–100 cm. This sampler was chosen because it minimizes soil compaction during sampling. Ten cores were collected per sampling period (n = 10).

In the field, bulk soil matrix was gently removed by washing samples through a 0.5-mm mesh sieve using river water. In the laboratory, remaining soil was removed by further washing through the same sieve using tap water. Roots were sorted manually into fine roots ($\leq$2 mm), coarse roots (>2 mm), and classified as live or dead following Poungparn et al. [61]. All root samples were oven-dried at 70 °C for at least 48 h and weighed. Fine root biomass per unit ground area (g m^{-2}) at each depth was calculated from dry mass values and the sampler cross-sectional area.

2.4. Soil Sampling and Chemical Analyses

Soil sampling was conducted from 17–20 July 2025 within a 1.5-m radius of the root exudate sampling points at the upstream and midstream sites. Soil cores were collected from the surface (0–30 cm) and deep (30–60 cm) layers using a peat sampler (n = 5 per depth). Samples were sealed in plastic bags, transported to the laboratory at 4 °C, and stored refrigerated until analysis. Prior to analysis, samples were freeze-dried, passed through a 2-mm sieve, and finely ground using a vibrating mill. Soil pH and EC were measured using a pH/conductivity meter (LAQUA F-74, HORIBA, Kyoto, Japan) after mixing soil with deionized water (for pH(H_2O) and EC) or 1 M KCl (for pH(KCl)) at a soil-to-solution ratio of 1:5 and shaking for 1 h. Available inorganic N (NH_4^+ and NO_3^-) was extracted from moist soil (before freeze-drying). Soil (dry-weight-equivalent) was mixed with 2 M KCl solution at a soil-to-solution ratio of 1:10, shaken for 1 h, and filtered through Whatman No. 6 filter paper (Cytiva, Marlborough, MA, USA). NH_4^+ and NO_3^- concentrations in the extracts were determined using flow-injection analyzers (OG-FI-300 for NO_3^- and OG-FI-300NH for NH_4^+; Ogawa & Co., Ltd., Kobe, Japan).

To evaluate soil C and N storage forms, density fractionation was performed following Hamada et al. [57,62], separating soil organic matter into three fractions using a density cutoff of 1.6 g cm^{-3}: (1) the free light fraction (f-LF), consisting mainly of fresh plant residues; (2) the mineral-associated light fraction (m-LF), representing decomposed organic matter incorporated into aggregates or pores; and (3) the heavy fraction (HF), consisting of highly decomposed organic matter physically and chemically protected by soil minerals. Organic C and N contents of each fraction were measured using a CN analyzer (Sumigraph

NC-TR22, Sumika Chemical Analysis Service, Osaka, Japan). For the HF, inorganic carbon was removed by acid fumigation following Midwood and Boutton [63] prior to analysis.

2.5. Data Analysis

Means and standard errors (SEs) were calculated for root exudation rates, soil properties, and fine-root morphological data at each site. Differences in root exudation rates (Figure 2), soil physicochemical properties (Tables 1 and 2), incubation-solution parameters, and fine root biomass (Table A1) among sites were analyzed using one-way analysis of variance (ANOVA), followed by Tukey's HSD post hoc test where appropriate. Relationships between root exudation rates and ΔH^+ concentration, root N concentration, and root C:N ratio were tested using Pearson's correlation analysis (Figure 3a–c). Welch's *t*-tests were used to evaluate differences in root exudation rates between seasons within the same site, as well as differences in fine-root biomass and exudation rates between soil depths at the midstream site (Figure 4a,b). In addition, Welch's *t*-tests were used to evaluate differences in root exudation rates between all surface and deep soils (Figure 5a). All statistical analyses were performed using R Studio (version 2025.09.0-387).

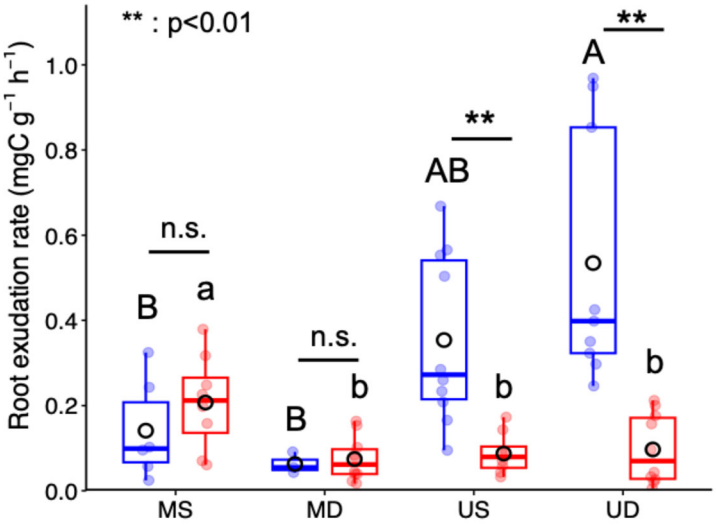


Figure 2. Boxplots of root exudation rates of *Bruguiera gymnorhiza* across different sampling points. Blue and red boxplots represent data collected in February 2025 (winter) and July 2025 (summer), respectively. Black circles indicate means, horizontal lines represent medians, boxes denote interquartile ranges, and whiskers extend to 1.5 × IQR. Sample sizes are provided in Section 3. Different letters (uppercase or lowercase) indicate significant differences among sampling points within the same season ($p < 0.05$), and asterisks (**) indicate significant seasonal differences within the same sampling point ($p < 0.01$). Abbreviations: MS, Midstream Surface (0–30 cm); MD, Midstream Deep (30–60 cm); US, Upstream Surface (0–30 cm); UD, Upstream Deep (30–60 cm); n.s., not significant.

Table 1. Soil physicochemical properties (mean ± SE, $n = 5$) at each site sampled in July 2025. Different letters indicate statistically significant differences between sites ($p < 0.05$).

Point	Depth (cm)	pH (H_2O)	pH (KCl)	EC (mS cm^{-1})	NO_3^- (μgN g soil^{-1})	NH_4^+ (μgN g soil^{-1})
Midstream	0–30	6.25 ± 0.05 ab	5.32 ± 0.19 a	6.59 ± 0.32 a	0.03 ± 0.00 a	9.20 ± 0.30 a
	30–60	6.15 ± 0.03 b	5.47 ± 0.08 a	6.83 ± 0.41 a	0.03 ± 0.01 a	9.58 ± 0.30 a
Upstream	0–30	6.28 ± 0.04 a	5.58 ± 0.05 a	6.76 ± 0.34 a	0.03 ± 0.00 a	10.73 ± 0.57 a
	30–60	6.32 ± 0.01 a	5.60 ± 0.01 a	6.09 ± 0.22 a	0.03 ± 0.00 a	9.80 ± 0.44 a

Table 2. Density fractions of soil organic matter at each site in July 2025 (mean ± SE, $n = 5$). Different lowercase letters indicate statistically significant differences among sites ($p < 0.05$). Abbreviations: f-LF, free low-density fraction; m-LF, mineral-associated low-density fraction; HF, high-density fraction.

	Midstream		Upstream	
	0–30 cm	**30–60 cm**	**0–30 cm**	**30–60 cm**
f-LF (mgC g soil^{-1})	16.60 ± 6.32 a	11.22 ± 1.74 a	10.97 ± 0.80 a	10.80 ± 0.84 a
m-LF (mgC g soil^{-1})	5.06 ± 0.89 a	4.87 ± 0.42 a	7.12 ± 0.76 a	4.90 ± 0.28 a
HF (mgC g soil^{-1})	6.85 ± 1.00 a	5.24 ± 0.38 a	7.97 ± 0.90 a	7.79 ± 0.83 a
f-LF (mgC g soil^{-1})	0.38 ± 0.16 a	0.23 ± 0.04 a	0.26 ± 0.02 a	0.22 ± 0.02 a
m-LF (mgC g soil^{-1})	0.15 ± 0.03 a	0.13 ± 0.01 a	0.21 ± 0.03 a	0.12 ± 0.01 a
HF (mgC g soil^{-1})	0.49 ± 0.06 ab	0.37 ± 0.02 b	0.59 ± 0.06 a	0.57 ± 0.05 ab
CN ratio				
f-LF	46.81 ± 1.78 a	50.84 ± 2.44 a	42.72 ± 1.91 a	49.50 ± 1.82 a
m-LF	33.51 ± 0.62 a	38.45 ± 2.46 a	36.72 ± 4.38 a	40.25 ± 3.77 a
HF	13.93 ± 0.50 a	14.08 ± 0.35 a	13.37 ± 0.32 a	13.66 ± 0.30 a

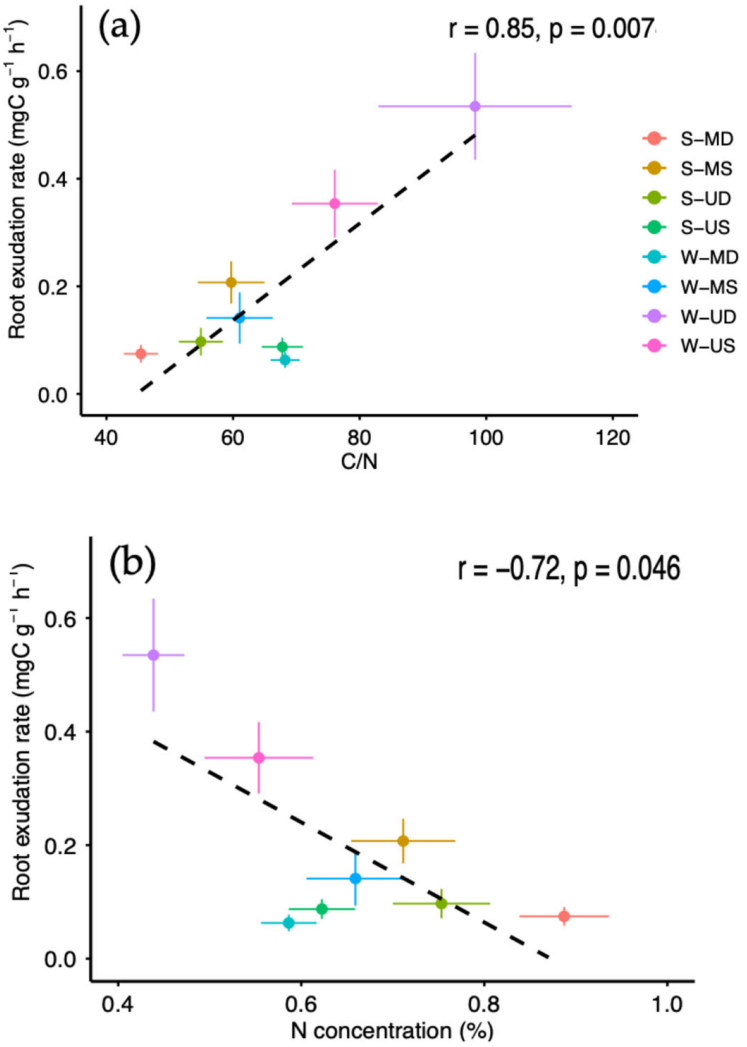


Figure 3. *Cont.*

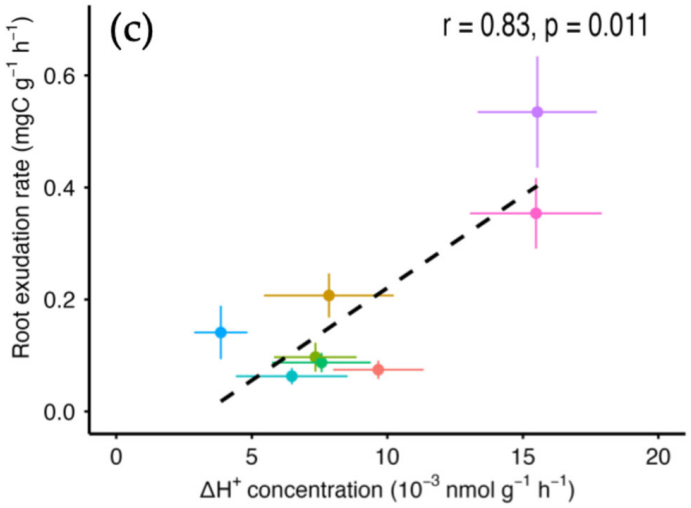


Figure 3. Pearson correlations between mean root exudation rates and (**a**) root C:N ratio, (**b**) root nitrogen concentration, and (**c**) ΔH^+ concentration across sampling points (mean ± SD, n = 8). r indicates the correlation coefficient and p indicates the significance level. Detailed data for root nitrogen concentration and C:N ratios are provided in Table A2. S and W denote Summer (July 2025) and Winter (February 2025), respectively. Abbreviations: MS, Midstream Surface; MD, Midstream Deep; US, Upstream Surface; UD, Upstream Deep.

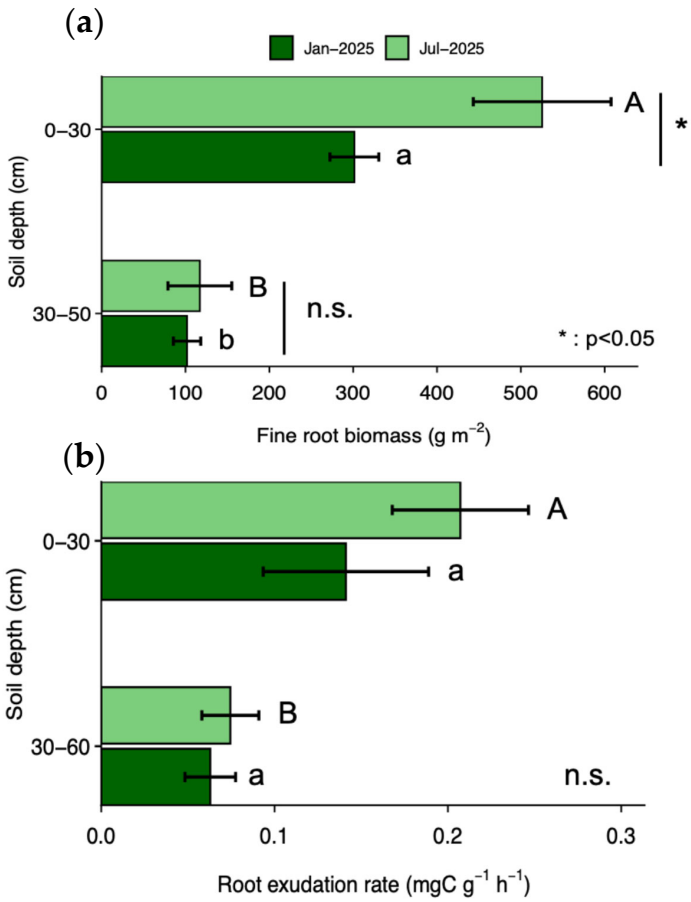


Figure 4. (**a**) Fine root biomass and (**b**) root exudation rates at the midstream site (mean ± SD). Fine root biomass for the 0–30 cm layer was calculated as the sum of the 0–15 cm and 15–30 cm layers. Different letters (uppercase or lowercase) indicate significant differences between soil depths within the same season ($p < 0.05$), and asterisks (*) indicate significant seasonal differences within the same soil depth ($p < 0.05$). Abbreviation: n.s., not significant.

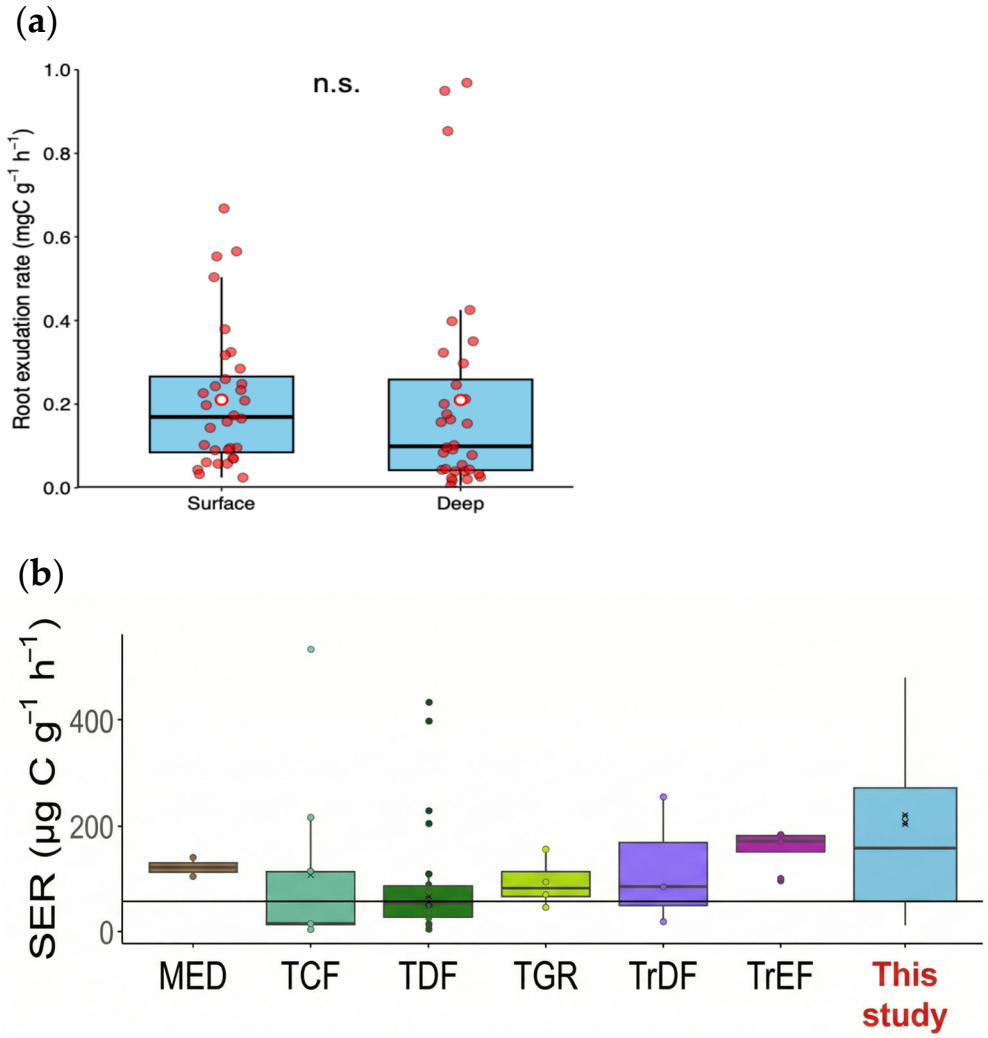


Figure 5. (**a**) Boxplots of root exudation rates of *Bruguiera gymnorhiza* in surface (0–30 cm) and deep (30–60 cm) soil layers, pooling data from the upstream and midstream sites. (**b**) Boxplots of specific exudation rate (SER) metadata across biomes based on the cuvette method of Phillips et al. [4], modified from Chari et al. [7], with the addition of root exudation rates of *B. gymnorhiza* obtained in this study (indicated in red). Abbreviations: MED, Mediterranean; TCF, temperate coniferous forest; TDF, temperate deciduous forest; TGR, temperate grassland; TrDF, tropical deciduous forest; TrEF, tropical evergreen forest; n.s., not significant. The horizontal line across panels in (**b**) indicates the geometric mean across all biomes. In all boxplots, open circles indicate means, horizontal lines represent medians, boxes denote interquartile ranges (IQR), and whiskers extend to 1.5 × IQR. Adapted with permission from Ref. [7]. Copyright 2024, The Authors.

3. Results

3.1. Experimental Conditions and Data Validation

The final sample sizes used for statistical analyses were as follows: During the winter campaign (February 2025), samples were collected from the midstream site (0–30 cm: $n = 6$; 30–60 cm: $n = 3$) and the upstream site (0–30 cm: $n = 10$; 30–60 cm: $n = 9$). During the summer campaign (July 2025), samples were collected from the midstream site (0–30 cm: $n = 8$; 30–60 cm: $n = 10$) and the upstream site (0–30 cm: $n = 9$; 30–60 cm: $n = 9$) (Figures 2–5; Tables A1 and A2). Variation in sample sizes mainly reflected losses caused by syringe displacement during high tides and removal of data where dissolved organic carbon (DOC) concentrations in treatment syringes were lower than in controls.

Across all sampling periods, the pH of the incubation solutions decreased significantly in the root-treatment syringes relative to the controls ($p < 0.05$; Table A1). Electrical

conductivity (EC) also decreased significantly, but only in the winter samples ($p < 0.05$; Table A1). Mean dry biomass of fine roots per syringe ranged from approximately 10–30 mg. Although these values were relatively low in the deep layers during winter ($p < 0.05$; Table A1), there were no order-of-magnitude differences across all sites and seasons.

DOC concentrations in field controls were significantly higher than those in initial laboratory controls only in the winter samples ($p < 0.05$; Table A1); however, the increase was small (<0.06 mg C syringe^{-1}), suggesting that any contamination by seawater intrusion during high tides had negligible impact on calculated exudation rates. In addition, DOC concentrations in foil-wrapped syringes (dark treatment) during July 2025 were within the range of values observed in unshaded syringes at the same depth and site, indicating that solar radiation had minimal effect on measured root exudation rates under our experimental conditions.

3.2. Root Exudation Rates and Relationships with Fine Root Chemistry and Proton Efflux

Across all samples, root exudation rates ranged from 0.01 to 0.97 mg C g^{-1} h^{-1}, with a mean of 0.22 ± 0.03 mg C g^{-1} h^{-1} (mean ± SE, $n = 64$) (Figure 2 and Table A2). In winter, no significant difference in exudation rate was observed between soil depths at the midstream site. However, rates at the upstream site tended to be higher than those at the midstream site, and a significant increase was observed in the deep layer (30–60 cm) relative to the midstream site ($p < 0.05$; Figure 2). In summer, exudation rates were highest in the surface layer (0–30 cm) at the midstream site ($p < 0.05$), whereas spatial variation between the two sites was less pronounced overall (Figure 2).

Seasonal comparisons revealed that exudation rates at the upstream site were significantly higher in winter than in summer, both in surface and deep layers ($p < 0.01$; Figure 2). When data were pooled across both seasons and both sites, there was no significant difference between exudation rates in surface and deep soils ($p > 0.05$; Figure 5a).

Mean root carbon concentration was approximately 40% in both seasons. In contrast, mean root nitrogen concentration was higher in summer (0.62–0.89%) than in winter (0.44–0.66%), resulting in generally lower C:N ratios in summer than in winter (Table A2). Mean exudation rates were significantly and positively correlated with mean root C:N ratio ($r = 0.85$, $p = 0.007$), and significantly and negatively correlated with mean root nitrogen concentration ($r = -0.72$, $p = 0.046$) (Figure 3a,b).

In addition, the rate of change in hydrogen ion concentration (ΔH^+; nmol $\times 10^{-3}$ g root^{-1} h^{-1}), calculated from pH differences between control and treatment syringes, showed a significant positive correlation with mean exudation rates ($r = 0.83$, $p < 0.05$; Table A2 and Figure 3c).

3.3. Relationships Between Fine Root Biomass and Root Exudation Rates

Fine root biomass (g m^{-2}; $n = 10$) at the midstream site was significantly higher in the surface layer (0–30 cm) than in the deep layer (30–50 cm) during both winter and summer ($p < 0.05$; Figure 4a). Furthermore, within the surface layer, fine root biomass was significantly greater in summer than in winter ($p < 0.05$; Figure 4a).

At the midstream site in summer, ANOVA followed by Tukey's tests detected no significant differences in exudation rate among depths (Figure 2). However, a Welch's *t*-test conducted specifically for the midstream site revealed significantly higher exudation rates in the surface than in the deep layer during summer ($p < 0.05$; Figure 4b).

Taken together, fine root biomass and root exudation rates at the midstream site showed parallel seasonal and vertical trends: both were higher in surface than in deep soils, and both increased from winter to summer in the surface layer (Figure 4a,b).

3.4. Soil Chemical Characteristics and Soil Organic Matter Fractions

Overall, no marked or systematic differences were observed in bulk soil pH, EC, or available nitrogen among the sampling sites (Table 1). On a finer scale, however, soil pH (H_2O) in the deeper layers of the midstream site was significantly lower than in the upstream site. Furthermore, available nitrogen (mainly NH_4^+) tended to be lower at the midstream site compared to the upstream site, with the lowest concentrations observed in the surface soil (Table 1).

Across the density fractions of soil organic matter (f-LF, m-LF, and HF), neither carbon contents nor C:N ratios differed significantly among sites ($p > 0.05$; Table 2). The carbon content of the f-LF fraction tended to be greatest in the surface soil at the midstream site, although this trend was not statistically significant. In contrast, the nitrogen content of the HF differed significantly among sites ($p < 0.05$; Table 2), with higher values at the upstream site than at the midstream site (Table 2).

4. Discussion

4.1. Relationships Between Root Exudation Rates, Soil Nutrient Availability, and Fine Root Morphological Traits

In the summer dataset, where both soil chemistry and root exudation data were available, a consistent pattern emerged despite the limited sample size ($n = 4$). Root exudation rates and fine root biomass were highest in the surface soil of the midstream site, where concentrations of available nitrogen—particularly ammonium (NH_4^+)—tended to be relatively low (Figures 2 and 4a,b, and Table 1). Although inter-site differences were not statistically significant at the 5% level ($p = 0.91$ for MS–MD, $p = 0.73$ for MS–UD, and $p = 0.08$ for MS–US), a tendency toward lower NH_4^+ availability was evident in the surface soil of the midstream site (Table 1). In terrestrial forests, trees are known to flexibly adjust belowground carbon allocation according to nutrient availability. Under nitrogen-limited conditions, trees often increase root exudation to stimulate rhizosphere microbial activity, thereby enhancing nutrient mobilization through the priming effect [9,23]. Conversely, root-derived carbon inputs tend to be suppressed where nutrients are abundant [64,65]. Because mangrove ecosystems typically experience nitrogen limitation, the combination of high exudation rates and low NH_4^+ concentrations observed in the midstream surface soil likely reflects an adaptive shift in belowground carbon allocation to support nutrient acquisition [45,66,67]. Furthermore, it has been reported that NH_4^+ and pH in mangrove soil water show a positive correlation [56]. The observed combination of low NH_4^+, low pH, and accelerated exudation at the MS site aligns well with this mechanism as an active physiological response to nutrient deficiency (Figure 4b and Table 1). This strongly suggests that mangroves may adopt a mutualistic nutrient acquisition strategy, actively manipulating their rhizosphere environment to fulfill specific nitrogen requirements.

In contrast, nitrogen concentrations in soil density fractions showed no clear relationship with root exudation rates (Table 1). This suggests that water-soluble and readily available nitrogen pools exert stronger control over root exudation than bulk soil nitrogen content. In addition, the strong positive relationship between root exudation rates and ΔH^+ concentration (Figure 3c) is consistent with the release of protons via dissociation of low-molecular-weight carboxylates—such as acetic, oxalic, and tartaric acids—known to be present in mangrove root exudates [51,52,68]. While elevated ΔH^+ concentrations may also be influenced by root respiration or microbial metabolism, the significant positive correlation with exudation rates suggests that organic acids are also a key contributing factor. Divalent carboxylates can chelate metal cations and enhance the solubility of otherwise recalcitrant phosphorus [10,15,69,70], implying that root exudation may facilitate the acquisition of both nitrogen and phosphorus. Collectively, these observations

support the interpretation that mangrove trees strategically regulate belowground carbon supply through fine-root biomass and exudation to optimize nutrient uptake under resource-limited conditions. Future advances will require integrated, larger-scale datasets combining exudate chemistry, nutrient dynamics, and fine root functional traits measured in situ.

A particularly notable result was the negative correlation between fine root nitrogen concentration and exudation, together with a positive relationship between exudation and root C:N ratio (Figure 3a,b). In terrestrial gymnosperms and angiosperms, the highest exudation rates are typically found in absorptive roots with high nitrogen content and high metabolic activity, whereas higher-order transport roots with greater lignification and higher C:N ratios generally show lower exudation [27,71,72]. Our findings contrast with this pattern. We propose that this discrepancy reflects physiological salt-adaptation mechanisms unique to mangrove trees [73]. Under saline conditions, mangrove roots accumulate compatible solutes, such as amino acids and sugars, within the cytoplasm to maintain osmotic balance [72–76]. These solutes may leak passively into the rhizosphere along osmotic gradients, even from structurally developed fine roots with high C:N ratios. However, because relationships between fine root traits and exudation vary widely among studies [77,78], it is likely that the highly dynamic, tidally driven soil environment further complicates these interactions in mangrove systems.

4.2. Carbon Allocation Between Fine-Root Biomass and Root Exudates

Photosynthetically derived carbon in trees is allocated belowground in two principal forms: fine root biomass and root exudates [2]. In mangrove forests, fine root production accounts for 30% of NPP, indicating a disproportionately large belowground allocation relative to most terrestrial forests. Approximately 65% of this production occurs in the upper 37 cm of the soil profile [38]. Consistent with these reports, we observed greater fine root biomass in the surface soil (0–30 cm) of the midstream site, accompanied by parallel variation in root exudation rates (Figure 4a,b).

This pattern is consistent with the hypothesized dual response of fine root biomass to soil redox status and sulfide toxicity [47,67,79]. While these parameters were not directly measured, it is well-established that prolonged tidal inundation can generate strongly reducing conditions in deeper soil layers, often accompanied by hydrogen sulfide accumulation via sulfate reduction. Elevated sulfide concentrations increase respiratory and maintenance costs for roots and can inhibit biomass investment [80]. In contrast, the more oxidative surface layer imposes lower physiological stress, potentially favoring carbon allocation to both fine root biomass and exudation. Indeed, the free light fraction (f-LF) of soil organic matter at this study site has been shown to originate from dead mangrove fine roots, as evidenced by C:N ratios and stable isotope signatures [57]. The relatively high f-LF content observed in the surface soil at the midstream site (Table 2) therefore reflects a substantial carbon investment into root biomass at this location.

Although we did not directly measure hydrological conditions or redox potential, seasonal differences in tidal range and site elevation almost certainly influenced hydroperiod and soil oxygen availability. The high fine root biomass in the surface soil at the midstream site suggests that enhanced metabolic activity, especially during summer, may promote carbon release as exudates. Conversely, the upstream site exhibited unusually high exudation rates in winter (Figure 2). As noted in Section 2, the high-tide levels during the sampling periods ranged from 104–154 cm in winter and 166–174 cm in summer. Consequently, the inundation duration, particularly at the upstream site, was likely shorter in winter than in summer. We hypothesize that this reduction in flooding potentially mitigated sulfide stress, thereby potentially allowing roots in deeper soil layers to maintain physiological activity.

Under such conditions, even during periods of reduced growth, roots may continue to release surplus carbon via exudation (see Section 4.3 for details). These findings indicate that belowground carbon allocation in mangrove forests is controlled by interacting gradients of hydroperiod, redox status, and nutrient availability, superimposed upon vertical variation in soil environment.

4.3. Root-Derived Carbon Exudation Fluxes in Mangrove Forests

In terrestrial forests, in situ measurements of root exudation using the cuvette-based method of Phillips et al. [4] are now well established, and recent meta-analyses have synthesized global patterns [7]. In mangrove forests, however, comparable quantitative data have been lacking. Our study provides the first such dataset for *B. gymnorhiza*, enabling direct methodological comparison with terrestrial systems.

Across all sampling depths and seasons, exudation rates in deep soils were similar to or higher than those in surface soils, and frequently approached the upper range reported for tropical forests [7] (Figure 5a,b). In most terrestrial forests, approximately 50% of fine-root biomass is concentrated in the top 20 cm [81], and both fine root biomass and exudation are typically greatest near the surface where nutrients, labile carbon, and microbial activity are highest [18,21,26]. Our results therefore challenge a key assumption derived from terrestrial systems and suggest that the drivers of belowground carbon allocation in mangroves fundamentally differ, likely driven by the characteristic vertical gradients of anoxia and sulfide stress associated with prolonged tidal flooding [82,83].

Temporal variation must also be considered. In terrestrial ecosystems, a trade-off has been proposed between fine-root growth and exudation, whereby exudation per unit root mass declines during periods of active growth and increases when growth slows [84,85]. Above-ground mangrove biomass (comprising litterfall and wood production) production generally peaks during warm, wet seasons [37], and similar seasonal trends occur on Ishigaki Island (Figure 1b). The elevated winter exudation rates observed at the upstream site may therefore reflect a shift in carbon allocation toward exudation during growth-limited periods. Future work should examine this hypothesis using continuous, year-round observations.

Mangrove roots often extend to depths of $\geq$1 m [41,43,44], and fine-root-derived organic matter has been detected in sediments deeper than 2 m [42]. These findings highlight the importance of deep-soil rhizosphere processes in mangrove carbon cycling [38]. When we integrated root-exudate carbon fluxes to 60 cm depth at the midstream site in winter, the annualized value reached approximately 0.4 kg C m^{-2} yr^{-1}. While we recognize this as a provisional estimate due to the uncertainties inherent in seasonal and spatial extrapolation, this value is notably higher than many reported fluxes from terrestrial forests [7]. Thus, our results provide preliminary evidence suggesting that root-derived carbon inputs could represent a significant, yet previously under-recognized, component of mangrove carbon budgets [36,38]. Incorporating such fluxes, even as tentative values, will be essential for refining future blue-carbon accounting frameworks.

4.4. Limitations and Future Perspectives

In the experimental setup of this study, artificial seawater was employed as the incubation medium. Consequently, compared to the conditions of actual soil interstitial water (pH $\approx$ 7.0, NH_4^+ < 1~mg/L), the pH was slightly higher (approximately 7.5; Table A1), and the concentration of NH_4^+—a primary nutrient—was nearly zero. It cannot be ruled out that these environmental discrepancies, particularly the nitrogen-deficient conditions, may have stimulated or inhibited exudation rates beyond those occurring in situ through the active physiological regulation of fine roots. However, given that NH_4^+ concentrations in

actual soil interstitial water are already extremely low (less than 1 mg/L), it is unlikely that such a difference would be sufficient to dramatically alter the order of magnitude of the observed exudation rates. Regardless, the cuvette-based method still has inherent limitations, and further refinement to better reflect field conditions remains essential.

Future research should expand the scope to include different tree species and stand ages, as well as deeper soil horizons beyond 60 cm. Furthermore, increasing the sampling frequency throughout the year will be crucial to capture detailed seasonal dynamics and more accurately constrain the spatiotemporal variability of root-derived carbon fluxes. Finally, while the present study evaluated exudates in terms of total organic carbon (TOC), identifying and quantifying primary chemical components is indispensable for a detailed understanding of their functional roles. To fully elucidate the biogeochemical processes within the mangrove rhizosphere, integrating both the quantity and quality of these exudates represents a critical challenge for future research.

5. Conclusions

This study provides the first in situ quantitative assessment of root exudation in a mangrove forest, addressing a major gap in belowground blue carbon research. Using a modified cuvette method in a subtropical *B. gymnorhiza* forest, we found that root exudation rates (0.01–0.97 mg C g^{-1} h^{-1}; mean: 0.22 mg C g^{-1} h^{-1}) were comparable to those reported for tropical terrestrial forests but exhibited clear spatial and seasonal variation. Exudation was closely associated with fine-root biomass under nitrogen-limited conditions at the midstream site, whereas unusually high rates occurred in deep soils during winter at the upstream site. Positive relationships between exudation rates, the root C:N ratio, and proton efflux further suggest links with stress-adaptation and nutrient-acquisition processes characteristic of mangrove environments. Integration of root-exudate fluxes to a depth of 60 cm yielded an estimated annual value of approximately 0.4 kg C m^{-2} yr^{-1}. Because fine-root systems extend well below 60 cm in mangrove forests, this value likely represents a conservative lower-bound estimate, indicating that root-derived carbon inputs are substantial and probably underrepresented in current mangrove carbon budgets. Our findings therefore support the view that root exudates constitute an important component of the "missing carbon" in mangrove ecosystems and should be incorporated into blue carbon assessments. Future research should expand in situ measurements across species and regions and integrate metabolomic and soil biogeochemical approaches to better constrain the role of root-derived carbon in mangrove carbon cycling.

Author Contributions: Conceptualization, Y.I.; validation, N.K., Y.I., and K.O.; formal analysis, N.K., K.O., and Y.I.; investigation, N.K., Y.I., T.O., and N.Y.; data curation, N.K., Y.I., K.O., and N.Y.; writing—original draft preparation, N.K.; writing—review and editing, N.K., K.O., T.O., N.Y., and Y.I.; project administration, T.O. and Y.I.; funding acquisition, T.O. and Y.I. All authors have read and agreed to the published version of the manuscript.

Funding: This research was supported by the Japan Society for the Promotion of Science KAKENHI (21KK0186) and Asahi Group Foundation (Y.I).

Data Availability Statement: Data is provided within the manuscript.

Acknowledgments: We thank the members of the Laboratory of Soil Science at The University of Shiga Prefecture and Ecosystem Ecology at Institute for Advanced Study, Gifu University for their discussion and sampling on this research. We would like to thank Tomotsune from Tamagawa University for his assistance with the drone photography. Additionally, we would like to express our gratitude to all other contributors who assisted with the site map creation.

Conflicts of Interest: The authors declare that they have no conflicts of interest.

Appendix A

Table A1. Water-quality parameters of the incubation solutions and fine-root biomass within 50-mL syringes after 24 h of in situ incubation (mean ± SD). Different lowercase letters indicate statistically significant differences among sites within the same season, including the controls ($p < 0.05$). The DOC control was used to assess contamination under field conditions, whereas the batch control was used to assess syringe-derived contamination by filling a syringe with 50 mL of fresh incubation solution and shaking it horizontally for 24 h. Asterisks (*) indicate significant differences between the field control and the batch control ($p < 0.05$).

Season	Point	Depth (cm)	pH	EC (mS cm^{-1})	Fine Root Biomass (mg)	DOC (mgC Syringe^{-1})
February 2025	Midstream	0–30	7.16 ± 0.21 b	27.28 ± 2.21 b	27.25 ± 12.31 a	
		30–60	7.01 ± 0.06 bc	28.80 ± 2.34 b	26.35 ± 8.05 ab	
	Upstream	0–30	6.88 ± 0.20 bc	33.60 ± 1.47 a	18.05 ± 6.44 ab	
		30–60	6.99 ± 0.11 c	35.13 ± 1.19 a	12.15 ± 4.76 b	
	Control		7.61 ± 0.04 a	32.70 ± 0.17 a		0.07 ± 0.02 *
July 2025	Midstream	0–30	7.15 ± 0.21 b	34.95 ± 1.54 a	10.51 ± 6.83 a	
		30–60	7.03 ± 0.11 b	33.71 ± 1.80 a	16.21 ± 9.18 a	
	Upstream	0–30	7.12 ± 0.08 b	35.07 ± 0.95 a	18.04 ± 11.58 a	
		30–60	7.06 ± 0.14 b	34.21 ± 1.81 a	19.88 ± 13.90 a	
	Control		7.47 ± 0.11 a	33.47 ± 1.72 a		0.02 ± 0.01
	Batch-control					0.01 ± 0.01

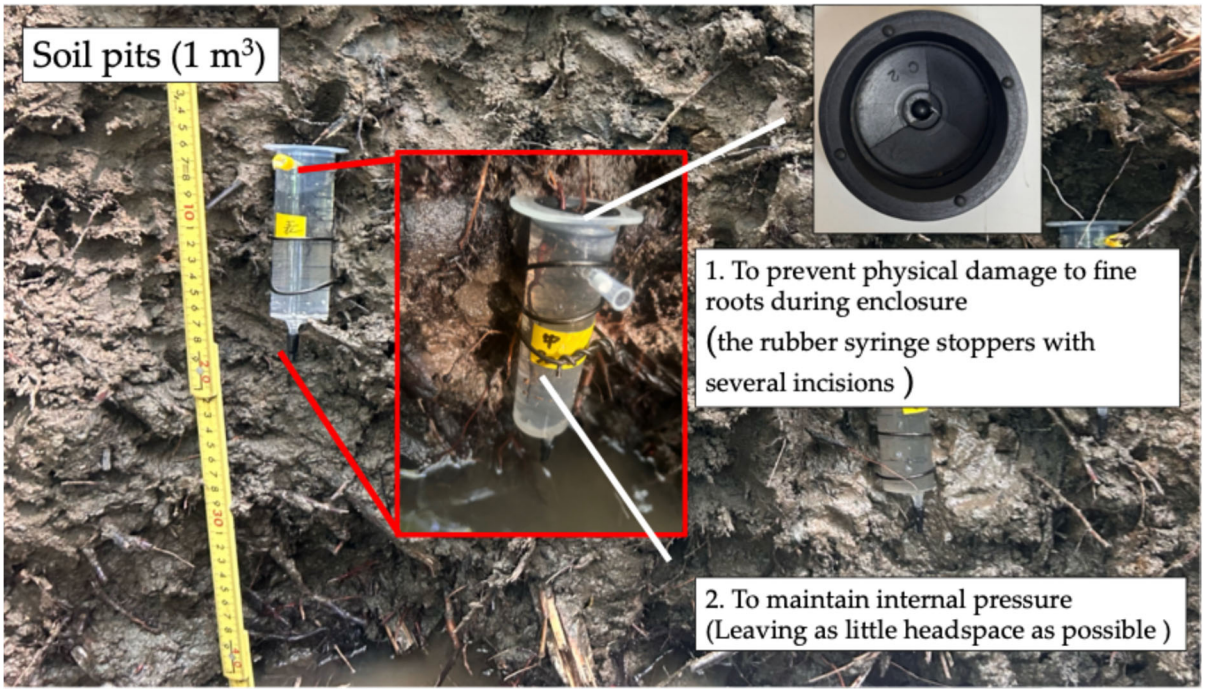


Figure A1. Quantification of root exudates in the field using the modified cuvette method employed in this study. Specific modifications are shown with photographs.

Table A2. Carbon and nitrogen contents of incubated roots, root exudation rates at each site, and root exudation flux at the midstream site (mean ± SE). FRB and REF represent fine root biomass and root exudation flux, respectively. REF was calculated by converting hourly root exudation rates to a daily basis and then multiplying these mean rates by the mean values of the corresponding fine root biomass. RE min and RE max represent the minimum and maximum root exudation rates, respectively.

Date	**February 2025**				**July 2025**				
Point	**Midstream**		**Upstream**		**Midstream**		**Upstream**		**All Data**
Depth (cm)	**0–30**	**30–60**	**0–30**	**30–60**	**0–30**	**30–60**	**0–30**	**30–60**	
Fine root C (%)	38.86 ± 0.34	39.87 ± 0.75	38.78 ± 0.64	39.13 ± 0.53	40.41 ± 0.24	39.18 ± 0.51	41.46 ± 0.39	39.51 ± 0.52	39.63 ± 0.21
Fine root N (%)	0.66 ± 0.05	0.59 ± 0.03	0.56 ± 0.06	0.44 ± 0.03	0.71 ± 0.06	0.89 ± 0.05	0.62 ± 0.03	0.77 ± 0.06	0.66 ± 0.02
Fine root CN	61.04 ± 5.25	68.23 ± 2.30	76.07 ± 7.16	98.24 ± 14.48	59.71 ± 5.27	45.45 ± 2.71	67.84 ± 2.87	53.44 ± 3.53	66.24 ± 3.23
RE min. (mgC g^{-1} h^{-1})	0.02	0.04	0.1	0.25	0.06	0.02	0.02	0.01	0.01
RE max. (mgC g^{-1} h^{-1})	0.32	0.09	0.67	0.97	0.38	0.16	0.17	0.21	0.97
RE (mgC g^{-1} h^{-1})	0.14 ± 0.05	0.06 ± 0.01	0.35 ± 0.06	0.53 ± 0.10	0.21 ± 0.04	0.07 ± 0.02	0.08 ± 0.02	0.11 ± 0.03	0.21 ± 0.03
RE (μgC g^{-1} h^{-1})	141.15 ± 47.70	62.91 ± 14.61	353.81 ± 63.00	534.63 ± 99.35	207.20 ± 39.30	74.49 ± 16.44	79.92 ± 16.93	105.52 ± 27.28	210.26 ± 27.30
FRB (g m^{-2})	301.43 ± 29.13	101.83 ± 16.28			525.46 ± 82.19	117.11 ± 38.05			
REF (gC m^{-2} day^{-1})	1.02	0.15			2.61	0.21			

https://doi.org/10.3390/f17020156

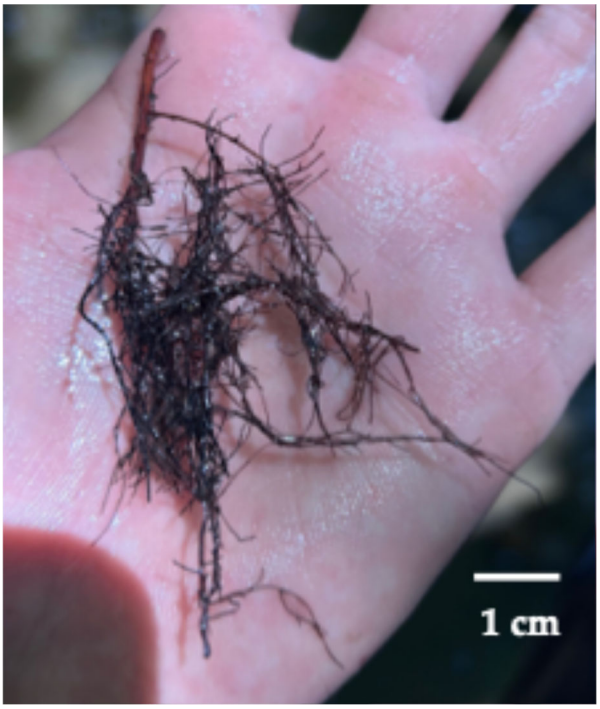


Figure A2. Morphological characteristics of fine roots of *Bruguiera gymnorhiza*.

References

1. Kannenberg, S.A.; Phillips, R.P. Plant responses to stress impacts: The C we do not see. *Tree Physiol.* **2017**, *37*, 151–153. [CrossRef]
2. Panchal, P.; Preece, C.; Peñuelas, J.; Giri, J. Soil carbon sequestration by root exudates. *Trends Plant Sci.* **2022**, *27*, 749–757. [CrossRef] [PubMed]
3. Jones, D.L.; Hodge, A.; Kuzyakov, Y. Plant and mycorrhizal regulation of rhizodeposition. *New Phytol.* **2004**, *163*, 459–480. [CrossRef]
4. Phillips, R.P.; Erlitz, Y.; Bier, R.; Bernhardt, E.S. New approach for capturing soluble root exudates in forest soils. *Funct. Ecol.* **2008**, *22*, 990–999. [CrossRef]
5. Aoki, M.; Fujii, K.; Kitayama, K. Environmental control of root exudation of low-molecular weight organic acids in tropical rainforests. *Ecosystems* **2012**, *15*, 1194–1203. [CrossRef]
6. Yin, H.; Wheeler, E.; Phillips, R.P. Root-induced changes in nutrient cycling in forests depend on exudation rates. *Soil Biol. Biochem.* **2014**, *78*, 213–221. [CrossRef]
7. Chari, N.R.; Tumber-Dávila, S.J.; Phillips, R.P.; Bauerle, T.L.; Brunn, M.; Hafner, B.D.; Klein, T.; Obersteiner, S.; Reay, M.K.; Ullah, S.; et al. Estimating the global root exudate carbon flux. *Biogeochemistry* **2024**, *167*, 895–908. [CrossRef]
8. Badri, D.V.; Vivanco, J.M. Regulation and function of root exudates. *Plant Cell Environ.* **2009**, *32*, 666–681. [CrossRef]
9. Kuzyakov, Y. Priming effects: Interactions between living and dead organic matter. *Soil Biol. Biochem.* **2010**, *42*, 1363–1371. [CrossRef]
10. Keiluweit, M.; Bougoure, J.J.; Nico, P.S.; Pett-Ridge, J.; Weber, P.K.; Kleber, M. Mineral protection of soil carbon counteracted by root exudates. *Nat. Clim. Change* **2015**, *5*, 588–595. [CrossRef]
11. Girkin, N.T.; Turner, B.L.; Ostle, N.; Sjögersten, S. Composition and concentration of root exudate analogues regulate greenhouse gas fluxes from tropical peat. *Soil Biol. Biochem.* **2018**, *127*, 280–285. [CrossRef]
12. Yang, Y.; Moorhead, D.L.; Craig, H.; Luo, M.; Chen, X.; Huang, J.; Olsen, J.E.; Chen, J. Differential responses of soil extracellular enzyme activities to salinization: Implications for soil carbon cycling in tidal wetlands. *Glob. Biogeochem. Cycles* **2022**, *36*, e2021GB007285. [CrossRef]
13. Wang, Q.; Yuan, Y.; Zhang, Z.; Liu, D.; Xiao, J.; Yin, H. Exudate components mediate soil C dynamic through different priming mechanisms in forest soils. *Appl. Soil Ecol.* **2021**, *160*, 103855. [CrossRef]
14. Chari, N.R.; Taylor, B.N. Soil organic matter formation and loss are mediated by root exudates in a temperate forest. *Nat. Geosci.* **2022**, *15*, 1011–1016. [CrossRef]
15. Wen, T.; Yu, G.H.; Hong, W.D.; Yuan, J.; Niu, G.Q.; Xie, P.H.; Sun, F.S.; Guo, L.D.; Kuzyakov, Y.; Shen, Q.R. Root exudate chemistry affects soil carbon mobilization via microbial community reassembly. *Fundam. Res.* **2022**, *2*, 697–707. [CrossRef]
16. Shabtai, I.A.; Hafner, B.D.; Schweizer, S.A.; Höschen, C.; Possinger, A.; Lehmann, J.; Bauerle, T. Root exudates simultaneously form and disrupt soil organo-mineral associations. *Commun. Earth Environ.* **2024**, *5*, 699. [CrossRef]

17. Brunn, M.; Mueller, C.W.; Chari, N.R.; Meier, I.C.; Obersteiner, S.; Phillips, R.P.; Taylor, B.; Tumber-Davila, S.J.; Ullah, S.; Klein, T. Tree carbon allocation to root exudates: Implications for carbon budgets, soil sequestration and drought response. *Tree Physiol.* **2025**, *45*, tpaf026. [CrossRef]
18. Tückmantel, T.; Leuschner, C.; Preusser, S.; Kandeler, E.; Angst, G.; Mueller, C.W.; Meier, I.C. Root exudation patterns in a beech forest: Dependence on soil depth, root morphology, and environment. *Soil Biol. Biochem.* **2017**, *107*, 188–197. [CrossRef]
19. Hicks Pries, C.E.; Sulman, B.N.; West, C.; O'Neill, C.; Poppleton, E.; Porras, R.C.; Castanha, C.; Zhu, B.; Wiedemeier, D.B.; Torn, M.S. Root litter decomposition slows with soil depth. *Soil Biol. Biochem.* **2018**, *125*, 103–114. [CrossRef]
20. Brunn, M.; Hafner, B.D.; Zwetsloot, M.J.; Weikl, F.; Pritsch, K.; Hikino, K.; Ruehr, N.K.; Sayer, E.J.; Bauerle, T.L. Carbon allocation to root exudates is maintained in mature temperate tree species under drought. *New Phytol.* **2022**, *235*, 965–977. [CrossRef] [PubMed]
21. Sakashita, R.; Hosoi, S.; Asakura, C.; Makita, N. Different patterns of fine-root exudation rates along soil depth of *Pinus densiflora*, *Chamaecyparis obtusa*, and *Cryptomeria japonica* in coniferous forests. *Rhizosphere* **2024**, *31*, 100946. [CrossRef]
22. Jakoby, G.; Rog, I.; Megidish, S.; Klein, T. Enhanced root exudation of mature broadleaf and conifer trees in a Mediterranean forest during the dry season. *Tree Physiol.* **2020**, *40*, 1595–1605. [CrossRef]
23. Chen, M.; Yao, X.; Cheng, H.; Fan, A.; Lin, R.; Wang, X.; Yang, Y.; Chen, G. Changes in Chinese fir plantations root exudation strategies seasonally and as tree age. *For. Ecol. Manag.* **2023**, *545*, 121239. [CrossRef]
24. Gao, Y.; Wang, H.; Yang, F.; Dai, X.; Meng, S.; Hu, M.; Kou, L.; Fu, X. Relationships between root exudation and root morphological and architectural traits vary with growing season. *Tree Physiol.* **2024**, *44*, tpad118. [CrossRef] [PubMed]
25. Sun, L.; Ataka, M.; Kominami, Y.; Yoshimura, K. Relationship between fine-root exudation and respiration of two *Quercus* species in a Japanese temperate forest. *Tree Physiol.* **2017**, *37*, 1011–1020. [CrossRef] [PubMed]
26. Meier, I.C.; Tückmantel, T.; Heitkötter, J.; Müller, K.; Preusser, S.; Wrobel, T.J.; Kandeler, E.; Marschner, B.; Leuschner, C. Root exudation of mature beech forests across a nutrient availability gradient: The role of root morphology and fungal activity. *New Phytol.* **2020**, *226*, 583–594. [CrossRef] [PubMed]
27. Sun, L.; Ataka, M.; Han, M.; Han, Y.; Gan, D.; Xu, T.; Guo, Y.; Zhu, B. Root exudation as a major competitive fine-root functional trait of 18 coexisting species in a subtropical forest. *New Phytol.* **2021**, *229*, 259–271. [CrossRef]
28. Hirano, Y.R.; Makita, N.; Hinokidani, K.; Aoyagi, R.; Imai, N. Species-specific root exudation responses to long-term phosphorus and nitrogen fertilization across successional status in Bornean tropical rainforests. *Ecosystems* **2025**, *28*, 47. [CrossRef]
29. Oburger, E.; Jones, D.L. Sampling root exudates—Mission impossible? *Rhizosphere* **2018**, *6*, 116–133. [CrossRef]
30. Alongi, D.M. Carbon cycling and storage in mangrove forests. *Annu. Rev. Mar. Sci.* **2014**, *6*, 195–219. [CrossRef]
31. Kida, M.; Fujitake, N. Organic carbon stabilization mechanisms in mangrove soils: A review. *Forests* **2020**, *11*, 981. [CrossRef]
32. Cooray, P.L.; Gregory, I.; Marcelus, G.; Chalmers, G.; Chittleborough, D. A review of properties of organic matter fractions in soils of mangrove wetlands: Implications for carbon storage. *Soil Biol. Biochem.* **2025**, *201*, 109660.
33. Alongi, D.M. Lateral export and sources of subsurface dissolved carbon and alkalinity in mangroves: Revising the blue carbon budget. *J. Mar. Sci. Eng.* **2022**, *10*, 1916. [CrossRef]
34. Reithmaier, G.M.S.; Cabral, A.; Akhand, A.; Bogard, M.J.; Borges, A.V.; Bouillon, S.; Burdige, D.J.; Call, M.; Chen, N.; Chen, X.; et al. Carbonate chemistry and carbon sequestration driven by inorganic carbon outwelling from mangroves and saltmarshes. *Nat. Commun.* **2023**, *14*, 8196. [CrossRef] [PubMed]
35. Alongi, D.M. Carbon cycling in the world's mangrove ecosystems revisited: Significance of non-steady state diagenesis and subsurface linkages between the forest floor and the coastal ocean. *Forests* **2020**, *11*, 977. [CrossRef]
36. Adame, M.F.; Cormier, N.; Taillardat, P.; Iram, N.; Rovai, A.; Sloey, T.M.; Yando, E.S.; Blanco-Libreros, J.F.; Arnaud, M.; Jennnerjahn, T.; et al. Deconstructing the mangrove carbon cycle: Gains, transformation, and losses. *Ecosphere* **2024**, *15*, e4806. [CrossRef]
37. Alongi, D.M. Global meta-analysis of mangrove primary production: Implications for carbon cycling in mangrove and other coastal ecosystems. *Forests* **2025**, *16*, 747. [CrossRef]
38. Arnaud, M.; Krause, S.; Norby, R.J.; Dang, T.H.; Acil, N.; Kettridge, N.; Gauci, V.; Ullah, S. Global mangrove root production, its controls and roles in the blue carbon budget of mangroves. *Glob. Change Biol.* **2023**, *29*, 3256–3270. [CrossRef]
39. Xiong, Y.; Liu, X.; Guan, W.; Liao, B.; Chen, Y.; Li, M.; Zhong, C. Fine root functional group based estimates of fine root production and turnover rate in natural mangrove forests. *Plant Soil* **2017**, *413*, 83–95. [CrossRef]
40. Bassar, A.T.M.Z.; Dannoura, M.; Okada, N.; Kamruzzaman, M. Fine root dynamics of *Kandelia obovata*, *Rhizophora stylosa* and *Bruguiera gymnorrhiza* in a mangrove environment in Okinawa, Japan. *Reg. Stud. Mar. Sci.* **2023**, *64*, 103046. [CrossRef]
41. Iimura, Y.; Kinjo, K.; Kondo, M.; Ohtsuka, T. Soil carbon stocks and their primary origin at mature mangrove ecosystems in the estuary of Fukido River, Ishigaki Island, southwestern Japan. *Soil Sci. Plant Nutr.* **2019**, *65*, 435–443. [CrossRef]
42. Kida, M.; Watanabe, I.; Kinjo, K.; Kondo, M.; Yoshitake, S.; Tomotsune, M.; Iimura, Y.; Umnouysin, S.; Suchewaboripont, V.; Poungparn, S.; et al. Organic carbon stock and composition in 3.5-m core mangrove soils (Trat, Thailand). *Sci. Total Environ.* **2021**, *801*, 149682. [CrossRef]

43. Lin, Q.; Chen, L.; Zhang, J.; Wang, L.; Yu, X.; Guo, Q. How fine root turnover functions during mangrove root zone expansion and affects belowground carbon processes. *Plant Soil* **2023**, *488*, 451–463. [CrossRef]
44. Ohtsuka, T.; Umnouysin, S.; Suchewaboripont, V.; Yimatsa, N.; Rodtassana, C.; Kida, M.; Iimura, Y.; Yoshitake, S.; Fujitake, N.; Poungparn, S. Biomass recovery of coastal young mangrove plantations in Central Thailand. *Sci. Rep.* **2024**, *14*, 11359. [CrossRef] [PubMed]
45. Arnaud, M.; Morris, P.J.; Baird, A.J.; Dang, H.; Nguyen, T.T. Fine root production in a chronosequence of mature reforested mangroves. *New Phytol.* **2021**, *232*, 1591–1602. [CrossRef]
46. Deborde, J.; Marchand, C.; Molnar, N.; Patrona, L.; Meziane, T. Concentrations and fractionation of carbon, iron, sulfur, nitrogen and phosphorus in mangrove sediments along an intertidal gradient (semi-arid climate, New Caledonia). *J. Mar. Sci. Eng.* **2015**, *3*, 52–72. [CrossRef]
47. Medina-Calderón, J.H.; Mancera-Pineda, J.E.; Castañeda-Moya, E.; Rivera-Monroy, V.H. Hydroperiod and salinity interactions control mangrove root dynamics in a karstic oceanic island in the Caribbean sea (San Andres, Colombia). *Front. Mar. Sci.* **2021**, *7*, 598132. [CrossRef]
48. Wang, F.; Xiao, K.; Santos, I.R.; Lu, Z.; Tamborski, J.; Wang, Y.; Yan, R.; Chen, N. Porewater exchange drives nutrient cycling and export in a mangrove-salt marsh ecotone. *J. Hydrol.* **2022**, *606*, 127401. [CrossRef]
49. Zhang, Y.; Xiao, L.; Guan, D.; Chen, Y.; Motelica-Heino, M.; Peng, Y.; Lee, S.Y. The role of mangrove fine root production and decomposition on soil organic carbon component ratios. *Ecol. Indic.* **2021**, *125*, 107525. [CrossRef]
50. Kumar, T.; Ray, S.; Brahmachary, R.L.; Ghose, M. Preliminary GC-MS analysis of compounds present in the root exudates of three mangrove species. *Acta Chromatogr.* **2009**, *21*, 117–125. [CrossRef]
51. Vazquez, P.; Holguin, G.; Puente, M.E.; Lopez-Cortes, A.; Bashan, Y. Phosphate-solubilizing microorganisms associated with the rhizosphere of mangroves in a semiarid coastal lagoon. *Biol. Fertil. Soils* **2000**, *30*, 460–468. [CrossRef]
52. Liu, B.; Wu, L.; Pan, P.; Li, R.; Lin, B. Response of root exudates of *Bruguiera gymnorrhiza* (L.) to exposure of polycyclic aromatic hydrocarbons. *Front. Environ. Sci.* **2022**, *9*, 787002. [CrossRef]
53. Zhuang, W.; Yu, X.; Hu, R.; Luo, Z.; Liu, X.; Zheng, X.; Xiao, F.; Peng, Y.; He, Q.; Tian, Y.; et al. Diversity, function and assembly of mangrove root-associated microbial communities at a continuous fine-scale. *npj Biofilms Microbiomes* **2020**, *6*, 52. [CrossRef]
54. Mei, K.; Liu, J.; Xue, L.; Xu, J.; Jiang, W.; Tan, Z.; Li, A.; Qu, J.; Yan, C. Stimulation of oxalate root exudate in arsenic speciation and fluctuation with phosphate and iron in anoxic mangrove sediment. *Mar. Pollut. Bull.* **2023**, *189*, 114823. [CrossRef]
55. Lei, Y.; Bi, Y.; Dong, X.; Li, H.; Gao, X.; Li, X.; Yan, Z. Effects of salinity on iron-organic carbon binding in the rhizosphere of *Kandelia obovata*: Insights from root exudate analysis. *Sci. Total Environ.* **2024**, *955*, 177214. [CrossRef]
56. Kato, N.; Osaka, K.; Ohtsuka, T.; Iimura, Y. Root exudates in mangrove forests accelerate bicarbonate production in the soil environment. *Sci. Rep.* **2024**, *14*, 31765. [CrossRef]
57. Hamada, K.; Yimatsa, N.; Ohtsuka, T.; Fujitake, N.; Miyajima, T.; Yokoyama, Y.; Miyairi, Y.; Kida, M. Organo-metal coprecipitation contributes to stable organic carbon fraction in mangrove soil. *CATENA* **2025**, *256*, 109075. [CrossRef]
58. Ohtsuka, T.; Tomotsune, M.; Suchewaboripont, V.; Iimura, Y.; Kida, M.; Yoshitake, S.; Kondo, M.; Kinjo, K. Stand dynamics and aboveground net primary productivity of a mature subtropical mangrove forest on Ishigaki Island, south-western Japan. *Reg. Stud. Mar. Sci.* **2019**, *27*, 100516. [CrossRef]
59. Kihara, Y.; Dannoura, M.; Ohashi, M. Estimation of fine root production, mortality, and decomposition by using two core methods and litterbag experiments in a mangrove forest. *Ecol. Res.* **2021**, *37*, 53–66. [CrossRef]
60. Deslouis, C.; Falaras, P.; Gil, O.; Jeannin, M.; Maillot, V.; Tribollet, B. Influence of clay on calcareous deposit in natural and artificial sea water. *Electrochim. Acta* **2006**, *51*, 3173–3180. [CrossRef]
61. Poungparn, S.; Charoenphonphakdi, T.; Sangtiean, T.; Patanaponpaiboon, P. Fine root production in three zones of secondary mangrove forest in eastern Thailand. *Trees* **2016**, *30*, 467–474. [CrossRef]
62. Hamada, K.; Ohtsuka, T.; Fujitake, N.; Miyajima, T.; Yokoyama, Y.; Miyairi, Y.; Kida, M. Functional organic matter components in mangrove soils revealed by density fractionation. *Soil Sci. Plant Nutr.* **2024**, *70*, 88–99. [CrossRef]
63. Midwood, A.J.; Boutton, T.W. Soil carbonate decomposition by acid has little effect on $\delta^{13}C$ of organic matter. *Soil Biol. Biochem.* **1998**, *30*, 1301–1307. [CrossRef]
64. Xiong, D.; Huang, J.; Yang, Z.; Cai, Y.; Lin, T.C.; Liu, X.; Xu, C.; Chen, S.; Chen, G.; Xie, J.; et al. The effects of warming and nitrogen addition on fine root exudation rates in a young Chinese-fir stand. *For. Ecol. Manag.* **2020**, *458*, 117793. [CrossRef]
65. Yang, L.; Li, T.; Li, X.; Wang, Y.; Wang, X. Nitrogen addition decreases root exudation of four temperate tree species seedlings, independent of the applied nitrogen form. *Plant Soil* **2024**, *498*, 637–650. [CrossRef]
66. Alongi, D.M. Nitrogen cycling and mass balance in the world's mangrove forests. *Nitrogen* **2020**, *1*, 167–189. [CrossRef]
67. Cormier, N.; Twilley, R.R.; Ewel, K.C.; Krauss, K.W. Fine root productivity varies along nitrogen and phosphorus gradients in high-rainfall mangrove forests of Micronesia. *Hydrobiologia* **2015**, *750*, 69–87. [CrossRef]
68. Jiang, S.; Xie, F.; Lu, H.; Liu, J.; Yan, C. Response of low-molecular-weight organic acids in mangrove root exudates to exposure of polycyclic aromatic hydrocarbons. *Environ. Sci. Pollut. Res.* **2017**, *24*, 12484–12493. [CrossRef]

69. Wang, Y.; Lambers, H. Root-released organic anions in response to low phosphorus availability: Recent progress, challenges and future perspectives. *Plant Soil* **2020**, *447*, 135–156. [CrossRef]
70. Mukai, M.; Aiba, S.; Kitayama, K. Effects of tree-root exudates on the solubilization of phosphorus adsorbed to non-crystalline minerals in the rhizosphere volcanic soils on Yakushima Island, Japan. *Trees* **2021**, *35*, 2031–2041. [CrossRef]
71. McCormack, M.L.; Dickie, I.A.; Eissenstat, D.M.; Fahey, T.J.; Fernandez, C.W.; Guo, D.; Helmisaari, H.S.; Hobbie, E.A.; Iversen, C.M.; Jackson, R.B.; et al. Redefining fine roots improves understanding of below-ground contributions to terrestrial biosphere processes. *New Phytol.* **2015**, *207*, 505–518. [CrossRef]
72. Akatsuki, M.; Makita, N. Influence of fine root traits on in situ exudation rates in four conifers from different mycorrhizal associations. *Tree Physiol.* **2020**, *40*, 1071–1079. [CrossRef] [PubMed]
73. Srikanth, S.; Lum, S.K.Y.; Chen, Z. Mangrove root: Adaptations and ecological importance. *Trees* **2016**, *30*, 451–465. [CrossRef]
74. Waditee, R.; Hibino, T.; Tanaka, Y.; Nakamura, T.; Incharoensakdi, A.; Hayakawa, S.; Suzuki, S.; Futsuhara, Y.; Kawamitsu, Y.; Takabe, T.; et al. Functional characterization of betaine/proline transporters in betaine-accumulating mangrove. *J. Biol. Chem.* **2002**, *277*, 18373–18382. [CrossRef]
75. Parida, A.K.; Jha, B. Salt tolerance mechanisms in mangroves: A review. *Trees* **2010**, *24*, 199–217. [CrossRef]
76. Krishnamurthy, P.; Mohanty, B.; Wijaya, E.; Lee, D.Y.; Lim, T.M.; Lin, Q.; Xu, J.; Loh, C.S.; Kumar, P.P. Transcriptomics analysis of salt stress tolerance in the roots of the mangrove *Avicennia officinalis*. *Sci. Rep.* **2017**, *7*, 10031. [CrossRef]
77. Weemstra, M.; Mommer, L.; Visser, E.J.W.; Van Ruijven, J.; Kuyper, T.W.; Mohren, G.M.J.; Sterck, F.J. Towards a multidimensional root trait framework: A tree root review. *New Phytol.* **2016**, *211*, 1159–1169. [CrossRef]
78. Robert, C.A.M.; Himmighofen, P.; McLaughlin, S.; Cofer, T.M.; Khan, S.A.; Siffert, A.; Sasse, J. Environmental and biological drivers of root exudation. *Annu. Rev. Plant Biol.* **2025**, *76*, 317–339. [CrossRef]
79. McKee, K.L. Soil physicochemical patterns and mangrove species distribution—Reciprocal effects? *J. Ecol.* **1993**, *81*, 477–487. [CrossRef]
80. Lamers, L.P.M.; Govers, L.L.; Janssen, I.C.J.M.; Geurts, J.J.M.; Van Der Welle, M.E.W.; Van Katwijk, M.M.; Van Der Heide, T.; Roelofs, J.G.M.; Smolders, A.J.P. Sulfide as a soil phytotoxin—A review. *Front. Plant Sci.* **2013**, *4*, 268. [CrossRef]
81. Finér, L.; Ohashi, M.; Noguchi, K.; Hirano, Y. Fine root production and turnover in forest ecosystems in relation to stand and environmental characteristics. *For. Ecol. Manag.* **2011**, *262*, 2008–2023. [CrossRef]
82. Lyimo, T.J.; Mushi, D. Sulfide concentration and redox potential patterns in mangrove forests of Dar es Salaam: Effects on *Avicennia Marina* and *Rhizophora Mucronata* seedling establishiment. *West. Indian Ocean J. Mar. Sci.* **2005**, *4*, 163–173. [CrossRef]
83. Qian, L.; Yu, X.; Gu, H.; Liu, F.; Fan, Y.; Wang, C.; He, Q.; Tian, Y.; Peng, Y.; Shu, L.; et al. Vertically stratified methane, nitrogen and sulphur cycling and coupling mechanisms in mangrove sediment microbiomes. *Mirobiome* **2023**, *11*, 71. [CrossRef]
84. Heinzle, J.; Liu, X.; Tian, Y.; Kwatcho Kengdo, S.; Heinze, B.; Nirschi, A.; Borken, W.; Inselsbacher, E.; Wanek, W.; Schindbacher, A. Increase in fine root biomass enhances root exudation by long-term soil warming in a temperate forest. *Front. For. Glob. Change* **2023**, *6*, 1152142. [CrossRef]
85. Prescott, C.E.; Grayston, S.J.; Helmisaari, H.S.; Kaštovská, E.; Körner, C.; Lambers, H.; Meier, I.C.; Millard, P.; Ostonen, I. Surplus carbon drives allocation and plant-soil interactions. *Trends Ecol. Evol.* **2020**, *35*, 1110–1118. [CrossRef] [PubMed]

Disclaimer/Publisher's Note: The statements, opinions and data contained in all publications are solely those of the individual author(s) and contributor(s) and not of MDPI and/or the editor(s). MDPI and/or the editor(s) disclaim responsibility for any injury to people or property resulting from any ideas, methods, instructions or products referred to in the content.